Liquid Crystal Binary Mixtures of 8OCB + 10OCB. Evidence for a Smectic A-to-Nematic Tricritical Point

Mohamed B. Sied, Sergio Diez, Josep Salud, David O. López,* Paul Cusmin, Josep Ll. Tamarit, and María Barrio

Laboratori de Caracterització de Materials (LCM), Departament de Física i Enginyeria Nuclear, ETSEIB Universitat Politècnica de Catalunya, Diagonal 647, 08028 Barcelona, Spain

Received: April 15, 2005; In Final Form: July 1, 2005

The two-component system octyloxycyanobiphenyl (8OCB) + decyloxycyanobiphenil (10OCB) has been studied by means of modulated differential scanning calorimetry as well as optical microscopy. The general trends of the phase diagram are similar to the two-component system octylcyanobiphenyl (8CB) + decylcyanobiphenil (10CB), previously published. Evidence for the existence of a TCP have been reported, the molar composition being about 0.33 of 10OCB. Additionally, the smectic mesophase of the 8OCB + 10OCB mixtures has been unmistakably characterized through optical measurements as smectic A for the whole composition range.

1. Introduction

Alkoxycyanobiphenyls (*n*OCB), where n corresponds to the number of methylenes in the substituent, are widely known as liquid crystal molecules, and their potential technical applications as electro-optical liquid crystal devices[1] as well as their photophysical properties[2,3] were and are extensively investigated. Likewise, some of these compounds ($n = 8$ and 9) display a smectic A (SmA)-to-nematic (N) transition for which, despite numerous studies, there is not yet experimental as well as theoretical consensus about the order of the transition.

One of the most convincing theories about the order of the SmA−N transition was exposed by Kobayashi,[4] McMillan,[5] and de Gennes[6] (denoted in the following as KMG theory). Assuming a coupling between nematic and smectic order parameters, the KMG theory is capable of predicting crossover behavior from the strict second-order 3D-XY transition, as well as the tricritical point (TCP) beyond which the first-order SmA-to-N transition occurs. In addition, the McMillan's ratio defined as T_{AN}/T_{NI} (T_{NI} is the nematic-to-isotropic transition temperature, and T_{AN} is the smectic-to-nematic transition temperature) accounts for that coupling. Its theoretical limit value for a TCP is 0.87, a value somewhat lower than the experimental values which range between 0.942 and 0.994.[7−14] In fact, the most experimental results about TCP are provided from two-component systems at ordinary pressure and the data do not seem to be universal, being strongly dependent on the materials.

Contrarily, Halperin, Lubensky, and Ma[15,16] published a theory, denoted as HLM theory, in which, as a general statement, a phase transition that is accompanied *by a screening of a massless field must be first-order in nature.* For the case of the smectic-to-nematic transition, taking into account that the role of *massless field* is played by transverse fluctuations of the nematic director, the HLM theory would predict a weak first-order SmA−N transition. Nevertheless, this fact has not yet been rigorously proved. Experimental studies in support of this theory were undertaken in the past decade of the twentieth century[17−20] and continue at present.[21−23] Most of these experimental studies are focused on the liquid-crystal homologues alkylcyanobiphenyls *n*CB (where *n* has the same meaning as for *n*OCB), to be precise, in octylcyanobiphenyl (8CB) as well as in the binary phase diagram for 8CB + decylcyanobiphenyl (10CB), which was built up by Marynissen et al.[7] as early as 1985, from very precise adiabatic scanning measurements. One of the most noticeable aspects of the early work of Marynissen et al. was the existence of a tricritical point (TCP) composition for the SmA-to-N transition. Nevertheless, Oweimreen,[21] for the first time, published that the SmA−N transition of 8CB is first-order in nature. Later Oweimreen and Hwang[22] republished the phase diagram for 8CB + 10CB obtained from density measurements using an Anton Paar densitometer and EPR spectroscopy to check the order of the SmA-to-N transition. As a relevant finding, Oweimreen and Hwang concluded that the SmA to N transition is first-order whatever the composition is. In addition, an induced smectic C-type structure for the mixtures 8CB + 10CB was reported. To check the controversy between KMG and HLM theories in relation to the order of the SmA−N transition in the binary phase diagram for 8CB + 10CB, some of the authors of the present paper prepared some mixtures and remeasured this binary phase diagram using the modulated differential scanning calorimetry (MDSC) technique.[10] In a recent work, two pieces of experimental evidence for the existence of a TCP composition have been provided. In addition, the induced smectic C-type structure for the mixtures 8CB + 10CB was completely discarded.

The SmA-to-N transition of octyloxycyanobiphenyl (8OCB) pure component was intensively studied in the past and has been studied at present by means of several experimental techniques: precise calorimetric measurements,[24−29] piezothermal studies,[30] X-ray measurements,[31,32] light-scattering studies,[33] volumetric measurements,[34] and elastic modulus and birefringence determinations.[35,36] Conflicting results on the order of the transition and the critical exponents have been reported.

Decyloxycyanobiphenyl (10OCB) has the same phase sequence as 10CB; that is, no nematic mesophase is displayed. So, one might expect that, in the same way as for the system

* To whom correspondence should be addressed. E-mail: david.orencio.lopez@upc.es.

10.1021/jp051957x CCC: $30.25
Published on Web 08/10/2005

8CB + 10CB, the binary system 8OCB + 10OCB, for which as far as we know it has not been published yet, constitutes a likely candidate to check the KMG and HLM theories in relation to the order of the SmA−N transition. In addition, the difference in the tail lengths of both pure 8OCB and 10OCB could induce an SmC-type structure as it was published by Oweimreen and Hwang[22] for binary mixtures of 8CB + 10CB.

In the work dealt with in this paper the purpose is then twofold: (i) to build up the binary phase diagram and to elucidate or not the existence of a TCP composition in the SmA-to-N transition and (ii) to elucidate the existence of a tilt-angle of the molecular axes in the mixtures 8OCB + 10OCB, taking advantage of the similarity with the binary system 8CB + 10CB, for which the existence of an induced SmC-type was proposed[22] and recently discarded.[10]

2. Experimental Section

2.1. Materials. The pure components 8OCB and 10OCB were synthesized and purified by Professor Dabrowski (Warsaw, Poland). By chromatography, the purity was stated to be higher than 99.9%, and no further purification was carried out. Liquid-crystal homogeneous binary mixtures of 8OCB + 10OCB were prepared at room temperature by weighing the pure components in sealed aluminum pans and heating to the isotropic phase in an ultrasonic bath for a period of several days.

2.2. MDSC Technique. The MDSC technique enables performing measurements such as conventional DSC as well as in modulated mode. This technique provides the ability to measure under suitable conditions (linear response and steady state) the specific heat at very slow underlying heating rates. Furthermore, by means of phase-shift ϕ measurements, MDSC provides a useful method to determine the order of the transition. This method, similar to that used in the AC technique[37−39] (δ being the AC-phase shift that is related to ϕ by the relationship $\delta = (\pi/2) - \phi$) has been recently proven to be very useful.[9] More details on the MDSC technique can be found elsewhere.[9,10,40,41]

The measurements consisted in heating the samples from smectic phase at 0.01 K·min^{-1}, with a modulation temperature amplitude of ±0.035 K and a period of 25 s. The sample masses were selected to ensure a uniform thin layer within the Al pans. The specific heat calibration was performed using pure synthetic sapphire.

2.2. Optical Microscopy. The microscopy observations were made with an Olympus polarizing microscope equipped with a Linkam THMSG-600 hot stage and a Linkam TMS-94 temperature controller. Two kinds of sample cells were used. One of them, from Linkam, with a thickness of 5 μm, and the other, from EHC, with a thickness of 25 μm, were filled by capillarity with the liquid crystal in its isotropic phase. The cooling and heating rates were 2 K·min^{-1}.

3. Results and Discussion

3.1. Smectic Structure in 8OCB + 10OCB Mixtures. It is well-known that both pure 8OCB and 10OCB display SmA mesophases, named *partial bilayer smectic*, currently denoted as SmA_d. In such mesophases, the smectic layer spacing d exceeds the molecular length l, such that $l < d < 2l$. What is not so clear is the smectic structure in the mixtures between both compounds. There was reported in other mixtures between smectogen A compounds[22] the possibility of an induced SmC structure. To study the smectic structure in 8OCB + 10OCB mixtures, optical experiments by means of a polarizing microscope have been performed. In Figure 1, the optical textures

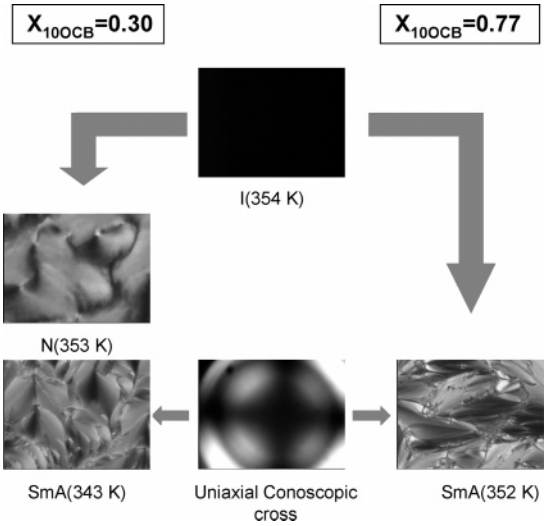

Figure 1. Sequence of photographs showing the textures for mixtures $X_{10OCB} = 0.30$ and 0.77 (in inhomogeneous alignment) at several temperatures. For homeotropic alignment, the uniaxial conoscopic cross in the smectic-mesophase, using a Bertrand lens, is shown.

for two different compositions ($X_{10OCB} = 0.30$ and 0.77) as examples, are shown at several temperatures. Both optical textures were obtained with EHC cells with the sample either in an inhomogeneous alignment or in a homeotropic alignment.

As for $X_{10OCB} = 0.30$, two different mesophases can be clearly observed on cooling the sample from isotropic I phase at about 354 K (an almost perfect black texture). The first one, at 353 K, shows a typical nematic-schlieren texture (in an inhomogeneous alignment) that is quite different from that observed for the SmC mesophase (gray-schlieren texture). The second one, at 343 K, seems to correspond to a fan-shaped texture (inhomogeneous alignment) compatible with a Sm-A structure. At the same temperature with the sample in an almost perfect homeotropic alignment, the uniaxial conoscopic cross using a Bertrand lens is clearly observed, pointing out the absence of biaxial optical properties and so the impossibility of a SmC structure. In addition the same behavior is observed as the crystal is formed.

As for $X_{10OCB} = 0.77$, only one mesophase can be identified on cooling the sample to 330 K. It seems to be that the sample transforms from I-phase (black texture) to a mesophase that in an inhomogeneous alignment does not show a nematic-schlieren texture (see photo at 352 K in Figure 1) but a texture closer to that obtained for 0.30 mole fraction at 343 K (the photo at the bottom of Figure 1, in which the fan-shaped texture of SmA is observed). Under homeotropic alignment, the uniaxial conoscopic cross through the Bertrand lens is undoubtedly obtained. So, as a conclusion, no nematic mesophase is observed for the 0.77 mole fraction.

Finally, to sum up, as we can see from Figure 1, for two representative compositions, no evidence of a SmC structure has been found. In addition, no evidence of a SmA-to-SmC transition has been observed at any composition.

3.2. Phase Diagram for 8OCB + 10OCB. As for pure 8OCB, the stable mesophase sequence on heating from room temperature is crystal(Cr)−SmA−N−I, whereas for pure 10OCB the N mesophase is absent, the mesophase sequence being Cr−SmA−I. As it has been cited before for 8OCB, the SmA-to-N transition has been recently reported by us as second-order in nature,[28,29] whereas the N to I is known to be first-order as a result of symmetry requirements.[42] For pure 10OCB, the SmA-to-I transition is also known to be first-order.[42] In Table 1, our

TABLE 1: Thermal Properties of Pure 8OCB and 10OCB for Mesophase Transitions

	SmA→N		N→I		
compound	T/K	ΔH/kJ·mol^{-1}	T/K	ΔH/kJ·mol^{-1}	ref
8OCB	340.37	<0.03	353.39	0.63	this work[a]

	SmA→I		
compound	T/K	ΔH/kJ·mol^{-1}	ref
10OCB	357.15		43
	357.45		44
	357.25	2.70	45
	357.13	3.31	46[b]
	357.02	1.34	this work

[a] A brief summary of the available thermal information on 8OCB from different bibliographic sources is available in refs 9 and 28. We have published our experimental results in refs 9 and 28. [b] DSC measurements at 5 K/min.

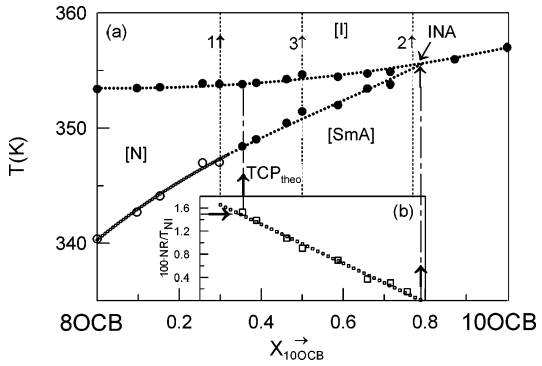

Figure 2. (a) Phase diagram for 8OCB+10OCB mixtures. (○○○) line and empty symbols correspond to second-order transition in nature. The (•••) line and solid symbols correspond to a first-order transition in nature. TCP_{theo} corresponds to the composition of TCP obtained from eq 4. (b) One hundred times the normalized nematic range (100NR/T_{NI}) against composition. The arrows numbered from 1 to 3 correspond to optical observations consigned in Figures 1 and 3.

thermal results of the mesophase transitions for these two compounds are reported.

In Figure 2a, the experimental phase diagram for 8OCB + 10OCB is shown. The points represent the temperatures for the SmA-to-N, N-to-I, and SmA-to-I mesophase transitions obtained by means of MDSC technique. The solid symbols correspond to a first-order phase transition, in contrast to the open symbols, which correspond to a second-order one. The solid (•••) line and open-symbol (○○○) line have the same meaning as for the symbols. It is important to realize that for a first-order transition a two-phase equilibrium exists although it is very narrow, and for simplicity, only one line has been drawn. In contrast, for a second-order in nature, no phase coexistence region exists and only a simple line must be drawn. The mesophase sequence was also evidenced optically by means of a polarizing microscope. The arrows 1 and 2 correspond to the compositions of Figure 1. In Figure 3, the optical measurements corresponding to the equimolar composition (marked in Figure 2a by the arrow 3) in a perfect parallel alignment using a Linkam cell are shown. The SmA mesophase can be clearly observed between 350 and 333 K, as can be inferred from the diagonal lines that correspond to the smectic planes.

In Figure 2b, 100 times the nematic range NR ($=T_{NI}-T_{AN}$) normalized by T_{NI} is plotted against composition. This value vanishes at the so-called *INA point* (the point at which I, N, and SmA mesophases would coexist). In fact, the INA point is truly a very small horizontal line (peritectic invariant) in which

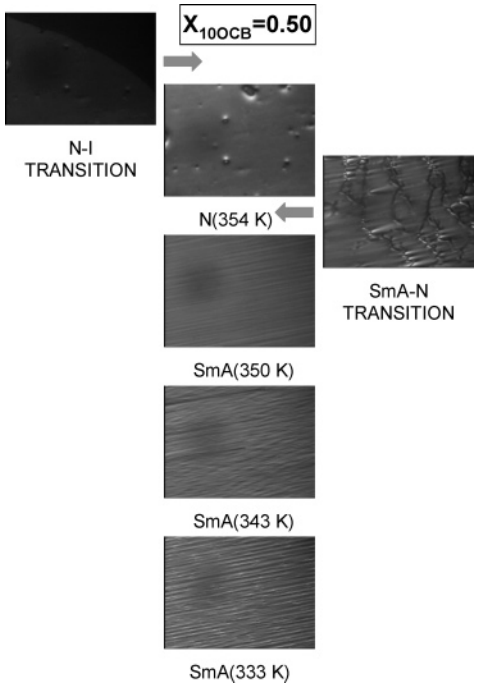

Figure 3. Sequence of photographs showing the textures for the mixture $X_{10OCB} = 0.50$ (in perfect parallel alignment) at several temperatures.

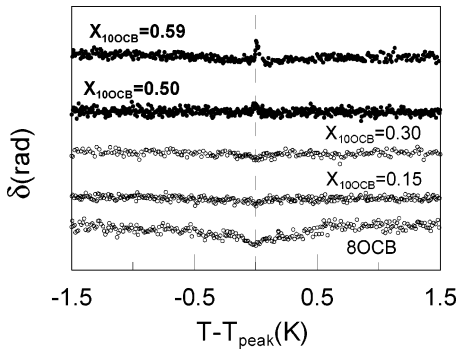

Figure 4. Comparison of the δ-phase shift data against ($T - T_{peak}$) near the SmA−N transition for pure 8OCB and for several mixtures of 8OCB + 10OCB. Solid symbols correspond to a first-order transition in nature. The δ data have been shifted in order to facilitate comparison.

these three mesophases coexist, but by simplicity only one simple point is drawn.

The second-order character of some mixtures at the SmA-to-N transition has been proven, in a first step, by means of δ-phase shift data through the transition. Values of δ against temperature for a representative number of mixtures 8OCB + 10OCB and for pure 8OCB are shown in Figure 4. The occurrence of a weak first-order transition can be detected by a peak in the value of δ, associated with the existence of a latent heat, as we can observe at the top of the Figure 4, for the mixtures $X_{10OCB} = 0.50$ and 0.59. Otherwise, for a second-order transition, a smooth dip or no changes in δ vs T through the phase transition are experimentally detected. At the bottom of Figure 4, pure 8OCB and mixtures up to 0.30 in mole fraction of 10OCB are representative examples of second-order SmA-to-N phase transition. This means that the order of the SmA-to-N transition must change between $X_{10OCB} = 0.30$ and $X_{10OCB} = 0.50$, and therefore, a TCP composition located between such values should exist.

To obtain a more accurate location of the TCP composition and also to provide other facts supporting the second-order

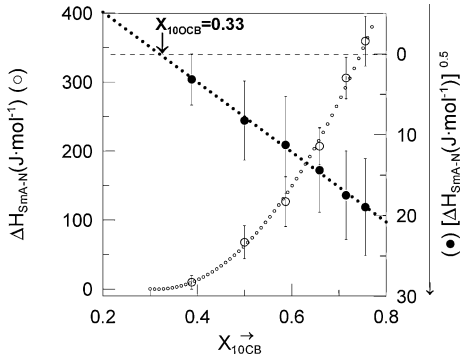

Figure 5. Latent heat ΔH_{SmA-N} (○) and $[\Delta H_{SmA-N}]^{1/2}$ (●) against composition for several mixtures of 8OCB + 10OCB.

character of the low-composition side of the SmA-to-N transition in 8OCB + 10OCB mixtures, the latent heat ΔH_{SmA-N} has been determined. It should be noticed that the latent heat associated with a first-order discontinuity in the enthalpy has been proven to be difficult to obtain with the required accuracy. For a given experiment, it is important to define the total enthalpy change:

$$\Delta H^{TOT}_{SmA-N} = \Delta H_{SmA-N} + \int \Delta C_p \, dT \qquad (1)$$

where the last term of the right-hand of the eq 1 is the pretransitional fluctuation contribution ($\Delta C_p \equiv C_p - C_p$-(background) is the excess specific heat due to the change in ordering that is associated with the transition). If a phase transition is of second order, the latent heat ΔH_{SmA-N} vanishes. The MDSC technique enables the determination in a direct manner of both right-hand terms in eq 1. In Figure 5, the latent heat of the SmA−N transition (empty symbols) decreases drastically when X_{10OCB} decreases, being zero at the tricritical composition. As it was pointed out by Thoen and co-workers,[7,47] when the $(\Delta H_{SmA-N})^{0.5}$ vs composition is plotted, a linear relationship is obtained (solid symbols in Figure 5). Linear fit of the $(\Delta H_{SmA-N})^{0.5}$ data (solid (•••) line in Figure 5) is a simple way of extrapolating the TCP composition, being located at $X_{10OCB} \approx 0.33$ (the error quoted from the fitting procedure was about 0.04 in mole fraction).

3.3. SmA-to-N Transition Data Analysis. The specific heat data near the SmA-to-N second-order transition have been analyzed using the renormalization group expression[14]

$$C_p^{\pm} = B + E\epsilon + A^{\pm}|\epsilon|^{-\alpha}[1 + D^{\pm}|\epsilon|^{0.5}] \qquad (2)$$

where ± indicates above and below the transition. The temperature at which smectic and nematic behaviors diverge is the critical temperature, T_c. The reduced temperature is $\epsilon(=(T - T_c)/T_c)$. The corresponding amplitudes above and below are $A^{\pm}$, whereas the constants B and E account for the specific heat background, both being above and below the transition. The specific heat critical exponent is α, also the same above and below the transition. The first-order correction to the scaling term is $D^{\pm}|\epsilon|^{0.5}$, which has been added to the simple power law expression to guarantee the smooth variation of the background at T_c. We have fixed the exponent of this term at the value 0.5 predicted for the 3D-XY model, and no additional fit was tried. The theory for the 3D-XY universality class predicts an amplitude ratio (A^-/A^+) of 0.971, a critical exponent α of −0.007, and (D^-/D^+) around unity. These predictions are different around the TCP, where the theoretical amplitude ratio of (A^-/A^+) is about 1.6, the critical exponent α is 0.5, and (D^-/D^+) is close to 1.

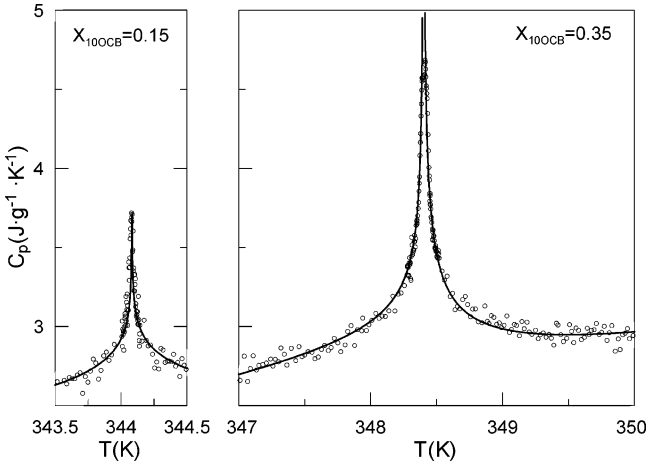

Figure 6. Experimental specific-heat data (○) and fit to eq 2 for the mixtures $X_{10OCB} = 0.15$ and 0.35 in the SmA-to-N phase transition (heating run). The parameter values are gathered in Table 2.

Equation 2 can be used for pure liquid crystals, whereas for mixtures one should measure $C_{p\phi}$ as a function of ϵ_ϕ, where constant ϕ designates a path of constant chemical potential difference. For mixtures of liquid-crystal homologues, the distinction between C_{pX} and $C_{p\phi}$ does not seem to be important as a consequence of the small values of $[dT_c/dX]_{TCP}$. The value for the slope at TCP in 8OCB + 10OCB is low enough (≅18 K), and Fisher renormalization, for which values of the slope at TCP should be around 200 K,[9] is not necessary. It is important to realize that the systems exhibiting Fisher renormalization usually involve polar and nonpolar compounds. So large differences in their chemical structure favor larger fluctuations of concentration.

The results of fits using eq 2 (α, A^-/A^*, D^-/D^+, T_c), over the range $|\epsilon| \leq 5 \times 10^{-3}$, are presented in Table 2 for pure 8OCB and for some mixtures of the two-component system 8OCB + 10OCB. All the parameter sets represent well enough the measured specific heat data, as indicated by χ^2 values. As an example, the results for two mixtures ($X_{10OCB} = 0.15$ and 0.35) are shown in Figure 6. The former was measured at a scanning rate of 0.01 K·min^{-1} and at a scanning rate 10 times lower in order to try to improve the evolution of the specific heat at temperatures nearer to the critical temperature. Both results were comparable. As for the $X_{10OCB} = 0.35$, it is interesting to note that this mixture seems tricritical with an α-value around 0.5 and (D^-/D^+) of about 1. As for its amplitude

TABLE 2: Results of Fits to Eq 2 for Pure 8OCB and for the Mixtures of 8OCB + 10OCB up to about the TCP Composition[a]

X_{10OCB}	N	α	A^-/A^+	D^-/D^+	T_c/K	$\chi^2 \times 10^3$
0 (8OCB)[b]	286	0.044 ± 0.002	1.01 ± 0.01	0.6 ± 0.2	340.37 ± 0.01	1
0.15[c]	760[d]	0.257 ± 0.006	1.09 ± 0.03	1.06 ± 0.01	344.08 ± 0.15	5
0.26	150	0.34 ± 0.03	1.29 ± 0.08	1.0 ± 0.2	346.99 ± 0.08	1.6
0.30	250	0.40 ± 0.01	1.06 ± 0.06	1.0 ± 0.3	347.03 ± 0.03	4.5
0.35	309	0.47 ± 0.01	0.73 ± 0.08	1.10 ± 0.02	348.40 ± 0.02	2

[a] N is the number of data points included in these fits. The errors quoted are the statistical uncertainties. [b] Parameter values are published in ref 9. [c] The best fit values were obtained over the range $|\epsilon| \leq 1.5 \times 10^{-3}$. [d] The scanning rate was 0.001 K·min^{-1}.

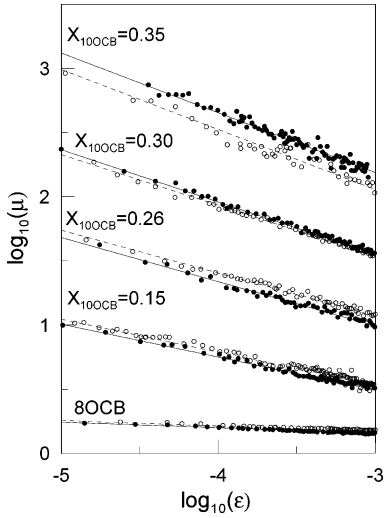

Figure 7. Double logarithmic plot for the parameter μ vs reduced temperature ϵ for pure 8OCB and all analyzed mixtures for N (●) and SmA (○) mesophases. Solid and dashed lines correspond to the fit using eq 2.

ratio (A^-/A^+), it deviates from the theoretical value, pointing out some kind of very small discontinuity at the transition, and thus the true TCP composition should be slightly lower than 0.35, as it could be concluded from Figure 5.

From eq 2, we can define the parameter μ as follows:

$$\mu = \frac{C_p^{\pm} - B - E\epsilon}{1 + D^{\pm}|\epsilon|^{0.5}} = A^{\pm}|\epsilon|^{-\alpha} \qquad (3)$$

Thus in a double logarithmic plot a linear relationship, with slope $-\alpha$, is found between the parameter μ and ϵ. To better observe the goodness of the fits, in Figure 7 we have displayed in this way μ and ϵ for pure 8OCB and all the analyzed mixtures. We observe a decreasing of the effective α values from $X_{10OCB} = 0.35$ to 8OCB. It should be noted the existence of two sets of data points for each compound and mixture. The displacement corresponds to the different amplitude A above and below the transition. It is important to realize for 8OCB that the two sets of data points are practically coincident ($A^- \approx A^+$).

In a precedent paper,[29] a common trend that accounts for the crossover behavior of the SmA-to-N transition, from 3D-XY universality class to TCP, for the set of *n*CB and *n*OCB homologous compounds was proposed. This trend can be well-represented by the following empirical function:

$$\alpha = 397(\mathrm{NR}/T_{\mathrm{NI}})^2 - 40.5(\mathrm{NR}/T_{\mathrm{NI}}) + 1.02 \qquad (4)$$

in which the α-specific heat critical exponent is parametrized as a function of the nematic range NR normalized by T_{NI} ($\mathrm{NR}/T_{\mathrm{NI}}$). It should be noticed that eq 4 does not account for the first-order behavior of the SmA-to-N transition, beyond the TCP. Nevertheless, eq 4 enables predicting the TCP composition in terms of the $\mathrm{NR}/T_{\mathrm{NI}}$ values on the second-order crossover behavior. In Figure 8b, the trend represented by eq 4 (○○○ line) is shown together with the effective α-values for the mixtures consigned in Table 2, for which their ($\mathrm{NR}/T_{\mathrm{NI}}$) are known from the phase diagram. In Figure 8a, at the same axis scale, $(\Delta H_{\mathrm{SmA-N}})^{0.5}$ is shown for the same first-order 8OCB + 10OCB mixtures consigned in Figure 5. An overall inspection of Figure 8 reveals two important facts: first, the effective α-values for the mixtures 8OCB + 10OCB are very well represented by eq 4, and second, a similar value of ($\mathrm{NR}/T_{\mathrm{NI}}$) at which TCP takes place is obtained irrespective of the representation is used (Figure 8a or Figure 8b).

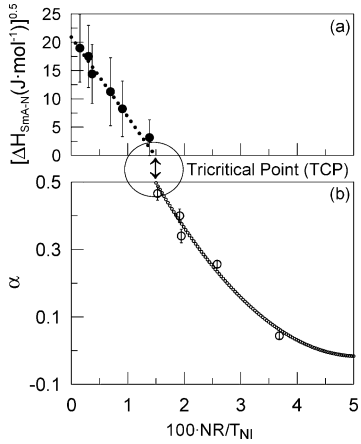

Figure 8. (a) Square-root latent heat ($[\Delta H_{\mathrm{SmA-N}}]^{1/2}$ (●)) and (b) effective critical exponent α against 100 times the normalized nematic range ($100\mathrm{NR}/T_{\mathrm{NI}}$). The (○○○) line represents the empirical trend given by eq 4.

4. Concluding Remarks

The phase diagram for 8OCB + 10OCB has been stated for the first time, as far as we know. The existence of a TCP composition for the SmA-to-N transition located at $X_{10OCB} \approx 0.33$ has been established. Two direct pieces of experimental evidence for such a result are reported: the data of the variation of the δ-phase shift with temperature and very accurate determinations of the latent heats as a function of composition. Likewise, the TCP composition has also been predicted through an empirical function that has been published elsewhere,[29] and that accounts for the order of the SmA-to-N transition in terms of a parameter, the ratio $\mathrm{NR}/T_{\mathrm{NI}}$, which is straightforwardly available when the two-component system has been stated.

On the other hand, the optical study of the smectic mesophase for two mixtures between 8OCB and 10OCB enables discarding a possible induced SmC structure.

Acknowledgment. The authors are grateful for financial support from the DGE (grant BFM2002-01425) and to the DURSI (grant SGR2002-00152). The authors are also indebt to C. Folcia (Departament de Física, UPV) for his help.

References and Notes

(1) Kirton, J.; Raynes, E. P. *Endeavour* **1973**, *32*, 71.
(2) Subramanian, R.; Patterson, L. K.; Levanon, H. *Chem. Phys. Lett.* **1982**, *93*, 578.
(3) Tamai, Y.; Yamazaki, I.; Masuhara, H.; Mataga, N. *Chem. Phys. Lett.* **1984**, *104*, 485.
(4) Kobayashi, K. *Phys. Lett.* **1970**, *31A*, 125.
(5) McMillan, W. L. *Phys. Rev. A* **1971**, *4*, 1238.
(6) de Gennes, P. G.; Prost, J. *The Physics of Liquid Crystals*; Oxford Science Publications, 1994.
(7) Marynissen, H.; Thoen, J.; van Dael, W. *Mol. Cryst. Liq. Cryst.* **1985**, *124*, 195.
(8) Marynissen, H.; Thoen, J.; van Dael, W. *Mol. Cryst. Liq. Cryst.* **1983**, *97*, 149.
(9) Sied, M. B.; Salud, J.; López, D. O.; Barrio, M.; Tamarit, J. Ll. *Phys. Chem. Chem. Phys. (PCCP)* **2002**, *4*, 2587.
(10) Lafouresse, M. C.; Sied, M. B.; Allouchi, H.; López, D. O.; Salud, J.; Tamarit, J. Ll. *Chem. Phys. Lett.* **2003**, *376*, 188.
(11) Huster, M. E.; Stine, K. J.; Garland, C. W. *Phys. Rev. A* **1987**, *36* (5), 2364.
(12) Stine, K. J.; Garland, C. W. *Phys. Rev. A* **1989**, *39* (6), 3148.

(13) Raja, V. N.; Prasad, S. K.; Rao, D. S. S.; Chandrasekhar, S. *Liq. Cryst.* **1992**, *12* (2), 239.
(14) Kumar, S. *Liquid Crystals: Experimental Study of Physical Properties and Phase Transitions*; Cambridge University Press, 2001.
(15) Halperin, B. I.; Lubensky, T. C.; Ma, S. *Phys. Rev. Lett.* **1974**, *32*, 292.
(16) Halperin, B. I.; Lubensky, T. C. *Solid State Commun.* **1974**, *14*, 997.
(17) Cladis, P. E.; van Saarloos, W.; Huse, D. A.; Patel, J. S.; Goodby, J. W.; Finn, P. L. *Phys. Rev. Lett.* **1989**, *62* (15), 1764.
(18) Anisimov, M. A.; Cladis, P. E.; Gorodetskii, E. E.; Huse, D. A.; Podneks, V. E.; Taratuta, V. G.; van Saarloos, W.; Voronov, V. P. *Phys. Rev. A* **1990**, *41* (12), 6749.
(19) Tamblyn, N.; Oswald, P.; Miele, A.; Bechhoefer, J. *Phys. Rev. E* **1995**, *51* (3), 2223.
(20) Yethiraj, A.; Bechhoefer, J. *Phys. Rev. Lett.* **2000**, *84* (16), 3642.
(21) Oweimreen, G. A. *J. Phys. Chem. B* **2001**, *105*, 8417.
(22) Oweimreen, G. A.; Hwang, J. S. *Chem. Phys. Lett.* **2001**, *334*, 83.
(23) Yethiraj, A.; Mukhopadhyay, R.; Bechhoefer, J. *Phys. Rev. E* **2002**, *65* (16), 3642.
(24) Johnson, D. L.; Hayes, C. F.; deHoff, R. J.; Shantz, C. A. *Phys. Rev. B* **1978**, *18* (9), 4902.
(25) Kasting, G. B.; Lushington, K. J.; Garland, C. W. *Phys. Rev. B* **1980**, *22* (1), 321.
(26) LeGrange, J. D.; Mochel, J. M. *Phys. Rev. Lett.* **1980**, *15* (1), 35.
(27) LeGrange, J. D.; Mochel, J. M *Phys. Rev. A* **1981**, *23* (6), 3215.
(28) Sied, M. B.; López, D. O.; Tamarit, J. Ll.; Barrio, M. *Liq. Cryst.* **2002**, *29* (1), 57.
(29) Sied, M. B.; Salud, J.; López, D. O.; Allouchi, H.; Díez, S.; Tamarit, J. Ll. *J. Phys. Chem. B* **2003**, *107* (24), 7820.
(30) Shashidar, R.; Ter Minassian, L.; Ratwa, B. R.; Kalkura, A. N. *J. Phys. (Paris) Lett*. **1982**, *43*, L239.
(31) Litster, D.; Als-Nielsen, J.; Birgenau, R. J.; Dana, S. S.; Davidov, D.; Garcia-Golding, F.; Kaplan, M.; Safinya, C. R.; Shaetzing, R. *J. Phys. (Paris) Colloq.* **1979**, *40*, C3−339.
(32) Birgenau, R. J.; Garland, C. W.; Kasting, G. B.; Ocko, B. M. *Phys. Rev. A* **1981**, *24* (5), 2624.
(33) Huang, C. C.; Pindak, R. S.; Ho, J. T. *Solid State Commun.* **1978**, *25*, 1015.
(34) Zywocinski, A.; Wieczorek, S. A.; Stecki, J. *Phys. Rev. A* **1987**, *36* (4), 1901.
(35) Benzekri, M.; Marcerou, J. P.; Nguyen, H. T.; Rouillon, J. C. *Phys. Rev. B* **1990**, *41* (13), 9032.
(36) Beaubois, F.; Claverie, T.; Marcerou, J. P.; Rouillon, J. C.; Nguyen, H. T. *Phys. Rev. E* **1997**, *56* (5), 5566.
(37) Garland, C. W. *Thermochim. Acta* **1985**, *88*, 127.
(38) Iannacchione, G. S.; Finotello, D. *Phys. Rev. E* **1994**, *50* (6), 4780.
(39) Castro, M.; Puértolas, J. A. *Thermochim. Acta* **1997**, *304/305*, 291.
(40) Wunderlich, B.; Boller, A.; Okazaki, I.; Kreitmeier, S. *Thermochim. Acta* **1996**, *282/283*, 143.
(41) Hatta, I.; Ichikawa, H.; Todoki, M. *Thermochim. Acta* **1995**, *267*, 83.
(42) Landau, L. D.; Lifshitz, E. M. *Statistical Physics*, Pergamon: Oxford, 1968.
(43) Brownsey, G. J.; Leadbetter, A. J. *Phys. Rev. Lett.* **1980**, *44* (24), 1608.
(44) Göbl-Wunsch, A.; Heppke, G.; Hopf, R. *Z. Naturforsh.* **1981**, *36a*, 213.
(45) Blachnik, N.; Kneppe, H.; Shneider, F. *Liq. Cryst.* **2000**, *27* (9), 1219.
(46) Oweimreen, G. A.; Morsy, M. A. *Thermochim. Acta* **2000**, *346*, 37.
(47) Thoen, J.; Marynissen, H.; van Dael, W. *Phys. Rev. Lett.* **1984**, *52* (3), 204.